

Zinc Complexation in Hydrothermal Chloride Brines: Results from *ab Initio* Molecular Dynamics Calculations

D. J. Harris* and J. P. Brodholt

Department of Geological Sciences, University College London, Gower Street,
London WC1E 6BT, U.K.

D. M. Sherman

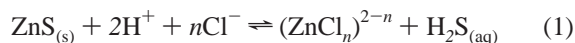
Department of Earth Sciences, University of Bristol, Wills Memorial Building, Queen's Road,
Bristol BS8 1RJ, U.K.

Received: May 10, 2002; In Final Form: November 20, 2002

We determined the coordination environment of Zn^{2+} in aqueous Cl^- brines at 25 °C and 300 °C using *ab initio* molecular dynamics simulations. The ZnCl^+ and ZnCl_2 complexes exist as pseudo-octahedral $\text{ZnCl}_m(\text{H}_2\text{O})_{6-m}$ clusters at 25 °C but occur as pseudo-tetrahedral $\text{ZnCl}_m(\text{H}_2\text{O})_{4-m}$ clusters at 300 °C. The ZnCl_3^- complex occurs as the pseudo-tetrahedral $\text{ZnCl}_3(\text{H}_2\text{O})^-$ cluster at 25 and 300 °C. The tetrahedral ZnCl_4^{2-} complex, however, is the dominant Zn–Cl complex at 25 °C, at least in highly concentrated (7.4 m) Cl^- brines. The change in hydration number with temperature for the ZnCl^+ and ZnCl_2 complexes will complicate extrapolations of solvation energies to hydrothermal conditions using a Born-model-based equation of state.

1. Introduction

The solubility of sphalerite (ZnS) in hydrothermal ore forming fluids is believed to result from the formation of chloride complexes of zinc:¹



Because of the n th order dependence of the chloride complexation, we need to know the speciation of Zn–Cl complexes as a function of composition, temperature, and pressure before we can quantitatively predict zinc solubilities. With increasing temperature, the dielectric constant of water decreases and the formation of higher order Zn–Cl complexes is favored. In the geochemical literature, extrapolations to hydrothermal conditions have been done using models based on the Born theory of solvation.^{2,3} Although useful, the continuum models fail to give us any real chemical insight on the nature of metal complexes in aqueous solution. Moreover, we cannot easily predict the formation of complexes for which there are no stability constant data at low temperature.

Experimental studies have postulated a large number of possible chlorozinc structures in aqueous solutions. These clusters include $\text{ZnCl}(\text{H}_2\text{O})_5^+$, $\text{ZnCl}_2(\text{H}_2\text{O})_2$, $\text{ZnCl}_2(\text{H}_2\text{O})_4$, $\text{ZnCl}_3(\text{H}_2\text{O})_2^-$, $\text{ZnCl}_3(\text{H}_2\text{O})^-$, and ZnCl_4^{2-} .^{1,4–10} As the list shows, the number of possible hydration structures around the zinc ion is large and uncertain.

A number of theoretical studies have attempted to throw some light on the structure of possible chlorozinc clusters;^{11,12} however, these studies have all been on the static structure in what is essentially a vacuum. The effect of the surrounding waters not in the first shell has not been included. To include

the effect of temperature and of the bulk electrolyte, an alternative method is to use *ab initio* quantum mechanical MD. The traditional MD approach is to use a *classical* model that describes the system in terms of pairwise interatomic potentials. However, this method is critically dependent upon the quality of the potential parameters used, and generating potentials for different environments can be very difficult. We have therefore decided to use *ab initio* MD where the forces at each time step are calculated using *ab initio* quantum mechanical techniques. Although modeling speciation in an aqueous solution is currently beyond the practical scope of the *ab initio* method due to the size of the system and the length of the simulation that would be required, it can be used to study the stability of individual clusters within a solution, or to calculate structural properties. We have used this approach to study some of the clusters predicted from the classical simulations. The aim is to predict which chlorozinc structures are likely to be stable in the solution, and to calculate their geometries in order to compare with, and help interpret, experimental data.

2. Modeling

The *ab initio* calculations were performed using the computer code CASTEP.¹³ This code employs density functional theory using a plane wave basis set with Vanderbilt ultrasoft pseudo potentials to approximate the interactions between core and valence electrons. The exchange–correlation energy was calculated using the Perdew–Burke–Ernzerhof (PBE) modification to the Generalized Gradient Approximation. Our plane-wave basis set had a cutoff of 380 eV. Increasing the cutoff above this value resulted in only a 1% change in the forces. The simulations were carried at constant volume and temperature (NVT), with the temperature controlled using a Nosé–Hoover thermostat.^{14,15}

We performed MD calculations on single clusters of zinc chloride in water. The cell size was chosen to be as large as

* Corresponding author. Tel.: +44 (0) 20 76793400. Fax: +44 (0) 20 73887614. E-mail: duncan.harris@ucl.ac.uk.

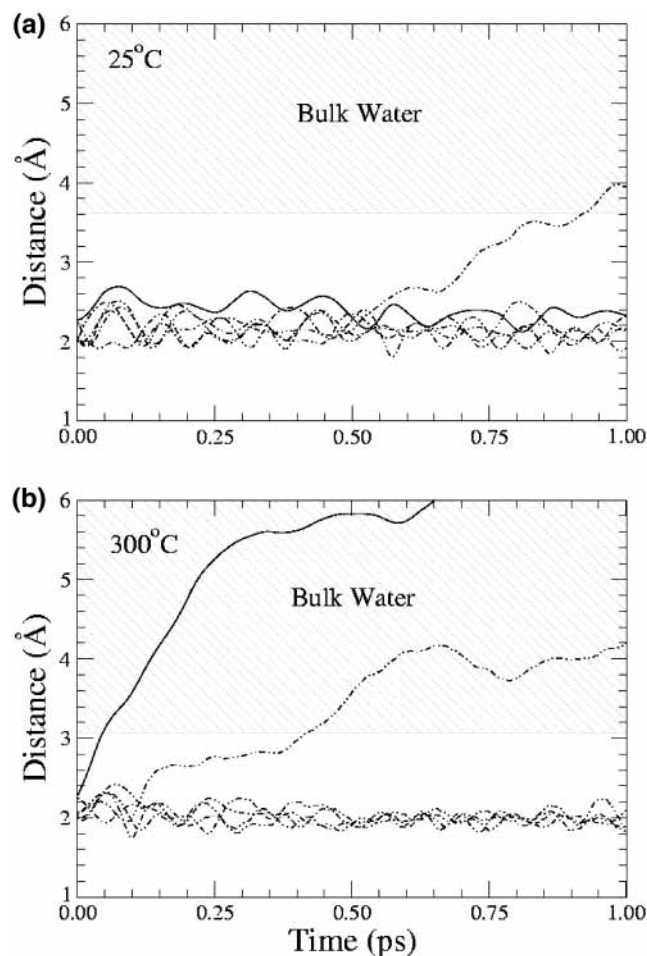


Figure 1. Calculated inter-ion distances for a $\text{ZnCl}(\text{H}_2\text{O})_5^+$ cluster as a function of time at (a) 25 °C and (b) 300 °C. Solid line = Zn–Cl, dash/dot = Zn–O(Cluster Water), shaded region = Zn–O(Bulk Water).

possible to prevent interactions between periodic images, while remaining small enough to allow for a reasonable calculation time. The cell size chosen contained 30 waters, 1 zinc ion, and a variable number of chloride ions, depending upon the system under consideration. A time step of 0.3 fs was required for the calculations. The cubic cell dimensions were fixed at the values for ambient conditions in all calculations, i.e., 10.39 Å for ZnCl^+ and ZnCl_2 , and 10.57 Å for ZnCl_3^- . An equilibrated structure was generated by performing 50 ps classical MD calculations using pair potentials.¹⁶ The resulting structure was then run in CASTEP for 0.1 ps before data were gathered.

3. Results

CASTEP calculations were performed to study the structure and dynamics of $\text{ZnCl}(\text{H}_2\text{O})_5$, $\text{ZnCl}_2(\text{H}_2\text{O})_4$, and $\text{ZnCl}_3(\text{H}_2\text{O})$ clusters.

3.1. ZnCl Hydration. Experimental studies on the structure of ZnCl^+ complexes at 25 °C are inconclusive as to whether the cluster is 4- or 6-coordinate. Work by Eastel et al.,⁸ using a combination of X-ray scattering, Raman, and EXAFS, concluded that the zinc in their samples was primarily tetrahedrally coordinated; however, this included contributions from higher order species such as ZnCl_2 and ZnCl_3^- . Maeda et al.¹⁰ used large-angle X-ray scattering and Raman spectra data to study various zinc clusters. They were not able to separate their concentrations of ZnCl^+ and ZnCl_2 , and therefore were not able to determine whether the cluster was 4- or 6-coordinate.

TABLE 1: Calculated Average Bond-Lengths at 25 °C and 300 °C

	25 °C		300 °C	
	Zn–Cl	Zn–O	Zn–Cl	Zn–O
ZnCl^+	2.51	2.17(5)		2.05(5)
ZnCl_2	2.38	2.17(8)	2.25	2.08(3)
ZnCl_3^-	2.34(7)	1.97	2.31(5)	2.01

Figure 1 shows plots of the inter-ion distances for a $\text{ZnCl}(\text{H}_2\text{O})_5$ cluster at 25 and 300 °C. The average bond distances are given in Table 1. Our Zn–Cl value of 2.51 Å is very high compared to the experimental value of 2.24 Å measured by Maeda et al.;¹⁰ however, the Zn–O distance of 2.17 Å agrees with the experimental value of 2.08–2.17 Å. It should be noted that the experimentally measured values of the Zn–Cl bond length were from a combination of ZnCl^+ , ZnCl_2 , and ZnCl_3^- clusters, whereas ours is from the ZnCl^+ only. At 25 °C there is no exchange of the water molecules or chloride ions in the cluster during the simulation. There is a very clear separation between the waters in the first hydration shell and the bulk waters. In the 300 °C calculation, however, the chloride ion is ejected early in the run; the water molecules remaining in the hydration shell reform into a trigonal bipyramidal arrangement. After 0.1 ps one of the waters in an axial position is lost, while the other four waters form a tetrahedral arrangement. Our calculations suggest, therefore, that at 25 °C this cluster should remain 6-coordinate, while at 300 °C the tetrahedral structure is likely. This is expected given the large entropy increase associated with the $\text{ZnCl}(\text{H}_2\text{O})_5 \rightarrow \text{ZnCl}(\text{H}_2\text{O})_3 + 2\text{H}_2\text{O}$ dehydration.

3.2. ZnCl₂ Hydration. Raman studies by Morris et al.⁵ at ambient conditions suggest an octahedral arrangement for ZnCl_2 clusters, and ab initio self-consistent-field molecular orbital calculations by Tossell¹¹ agreed with this conclusion. However, later calculations by Parchment et al.¹² concluded that a tetrahedral $\text{ZnCl}_2(\text{H}_2\text{O})_2$ cluster was preferred.

The average bond lengths are given in Table 1 at 25 and 300 °C. The calculated Zn–O bond lengths show good agreement at 25 °C with the data of Maeda et al.¹⁰ The Zn–Cl bond lengths are, again, much higher than those found by Maeda et al.¹⁰ Figure 2 shows the inter-ion distance plots for the $\text{ZnCl}_2(\text{H}_2\text{O})_4$ cluster. The chloride ions are initially in axial positions. In the 25 °C calculation, one of the equatorial waters is ejected from the cluster leaving a square pyramidal structure with a water at the apex. This structure remains stable for the remainder of the calculation. In the 300 °C calculation, one of the chloride ions is lost at the start of the run resulting in a square-based pyramidal structure with an apical chloride ion. At 0.2 ps into the calculation one of the basal water molecules is lost, producing a pseudo-tetrahedral structure.

The simulations suggest that an octahedral ZnCl_2 cluster is less stable than octahedral ZnCl , preferring a 5-coordinate structure at 25 °C and a pseudo-tetrahedral $\text{ZnCl}(\text{H}_2\text{O})_3^+$ structure at 300 °C.

3.3. ZnCl₃ Hydration. The $\text{ZnCl}_3(\text{H}_2\text{O})$ cluster at 25 °C (Figure 3a) remains stable throughout the duration of the calculation in a pseudo-tetrahedral configuration. Increasing the temperature to 300 °C has no effect on the stability (Figure 3b). ZnCl bond lengths of 2.34(7) are similar to the experimental value of 2.28 measured by Maeda et al.¹⁰ The obvious stability of the pseudo-tetrahedral structure of ZnCl_3^- also agrees well with the proposed experimental structure given by Maeda et al.¹⁰ They measured a Cl–Zn–Cl angle of 111° which is in

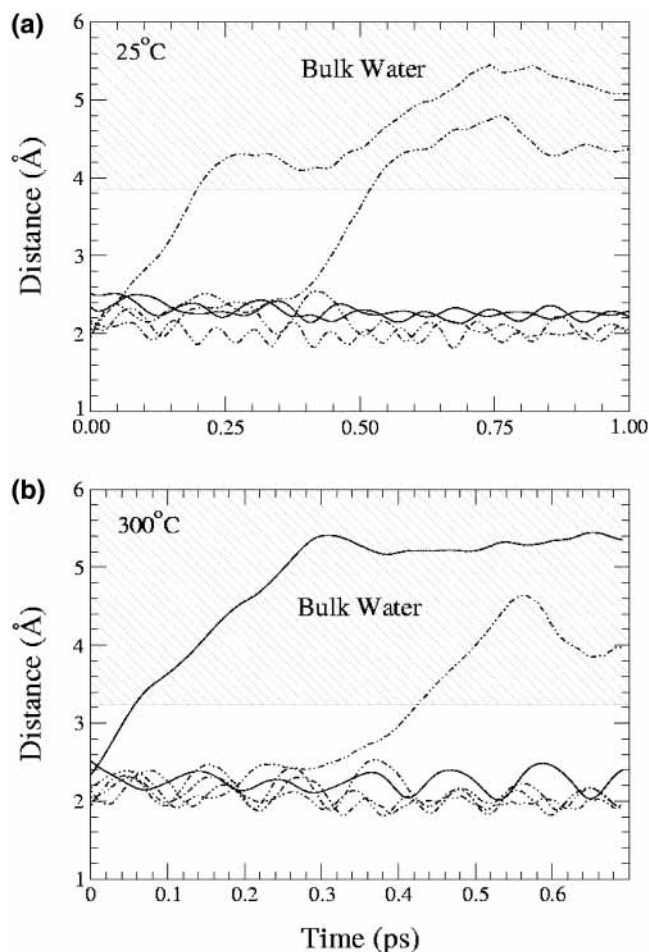


Figure 2. Calculated inter-ion distances for a $\text{ZnCl}_2(\text{H}_2\text{O})_4$ cluster as a function of time at (a) 25 °C and (b) 300 °C. Solid line = Zn–Cl, dash/dot = Zn–O_(Cluster Water), shaded region = Zn–O_(Bulk Water).

close agreement with our time-averaged value of 109.8°. Increasing the temperature has an insignificant effect on this angle.

3.4. Octahedral/Tetrahedral Transformations. Our calculations predict that the octahedral arrangement becomes unfavorable at higher temperatures and for clusters with greater numbers of chloride ions. Anderson et al.¹⁷ observed a similar effect when studying chlorozinc complexing in fluid inclusions with XAFS. Maeda et al.¹⁰ also concluded that ZnCl_4^{2-} would be tetrahedral. The change in structure from octahedral to pseudo-tetrahedral for the higher order clusters is due to the repulsion of the chloride charges. For clusters with three or four chlorides around a single zinc, the charges on the chloride ions force them to arrange themselves as far apart from each other as possible, ejecting any additional waters in the process. To demonstrate this we performed two CASTEP simulations of this rearrangement at 25 °C. We created a cell containing 30 waters, four chloride ions, and a single zinc ion. The cubic cell had dimensions of 10.40 Å. When four chloride ions and two of the water molecules are placed in an octahedral arrangement around the zinc ion, two arrangements are possible. Simulation A consisted of an equatorial placement of the four chloride ions with the waters at the axial positions (*trans*- $\text{ZnCl}_4(\text{H}_2\text{O})_2$), while simulation B consisted of three chlorides and a water molecule in equatorial positions and the other chloride and water at the axial positions (*cis*- $\text{ZnCl}_4(\text{H}_2\text{O})_2$) (Figure 4).

The cluster in simulation A rapidly lost one of the axial waters within 0.2 ps of the start of the calculation (Figure 5a). This

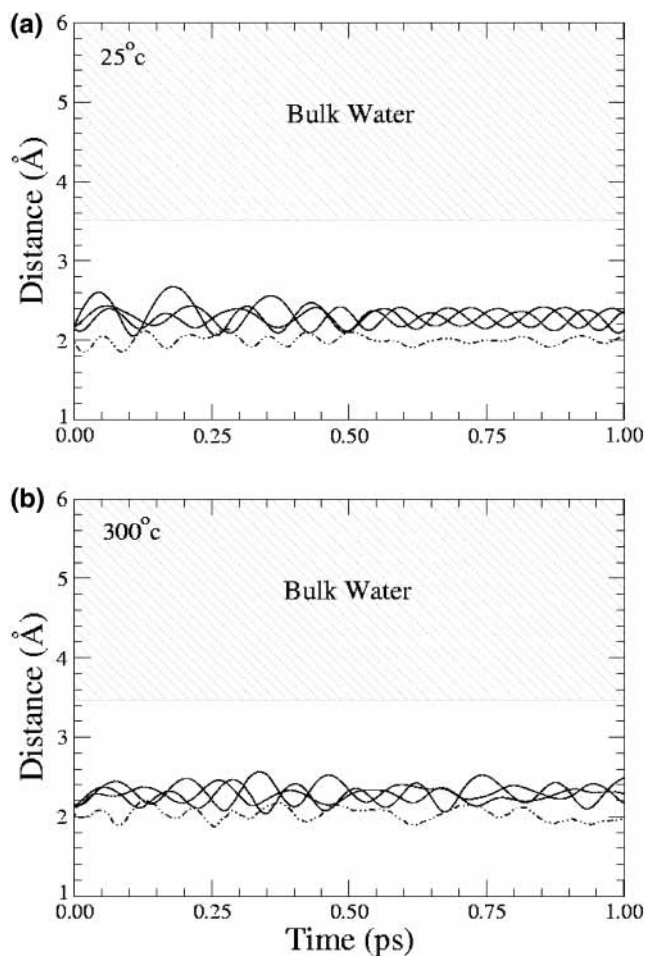


Figure 3. Calculated inter-ion distances for a $\text{ZnCl}_3(\text{H}_2\text{O})^-$ cluster as a function of time at (a) 25 °C and (b) 300 °C. Solid line = Zn–Cl, dash/dot = Zn–O_(Cluster Water), shaded region = Zn–O_(Bulk Water).

was accompanied by a very slight deformation of the chloride ions out of the equatorial plane, forming a distorted square-based pyramidal structure. During the following 0.4 ps one of the chloride ions was ejected, while the remaining structure reordered itself into a pseudo-tetrahedral structure.

The cluster in simulation B lost a water molecule after about 0.45 ps (Figure 5b), while the remaining 3 chloride ions in the same equatorial plane rearranged themselves to form a trigonal-bipyramidal structure, with an approximately 120 degree Cl–Zn–Cl equatorial angle. The remaining axial chloride moved away from the central zinc ion before returning and forcing out the axial water molecule. The whole structure then rearranged to give a tetrahedral ZnCl_4 cluster.

The different mechanisms of rearrangement in the two simulations can be explained in terms of charge proximity. In simulation A, the equatorial starting arrangement of the four chloride ions is very unfavorable. Although a water molecule is lost from the cluster very quickly, the chloride ions still remain in an approximate equatorial arrangement. To allow the charges to move away from each other to a more favorable distance, one of them is lost while the other three form a pseudo-tetrahedral arrangement around the zinc ion with the remaining water molecule.

In contrast, simulation B has only three chlorides in an equatorial arrangement, with the remaining chloride in an axial position. With the loss of the equatorial water, these chlorides are able to move farther away from each other. They are also forced out of plane by the axial chloride, and in the process the

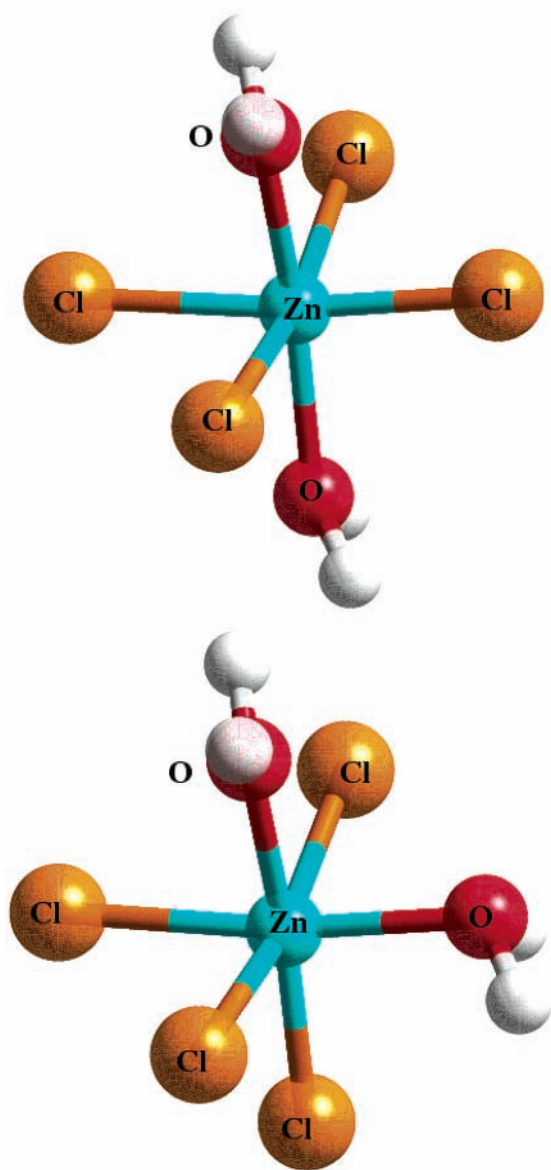


Figure 4. Starting arrangements for ZnCl_4 cluster calculations A and B.

remaining water is lost. This shows that a major factor in cluster formation is the charge proximity of the surrounding ligands. Despite the excess of chloride ions in solution, the formation of higher order clusters may be kinetically prevented as a result of the repulsion of approaching chloride ions by those ions already in the cluster.

4. Conclusions

Our calculations demonstrate that the octahedral structure is stable at low temperature and for clusters containing one or two chloride ions. For clusters with three or four chloride ions, the clusters will reform into a tetrahedral arrangement in order to minimize the repulsion between the charges.

The loss of ligands from around the zinc ion is facilitated by the increase in the entropy associated with the increased translational motion of these waters. However, there is also a drop in the dielectric constant of water as a result in the breakdown of hydrogen bonds. Previous experiments have shown that this will lead to a more charge-neutral solution, as chloride and zinc ions are less shielded from each other.^{1,9} Thus, these two factors should lead to an increase in the rate of

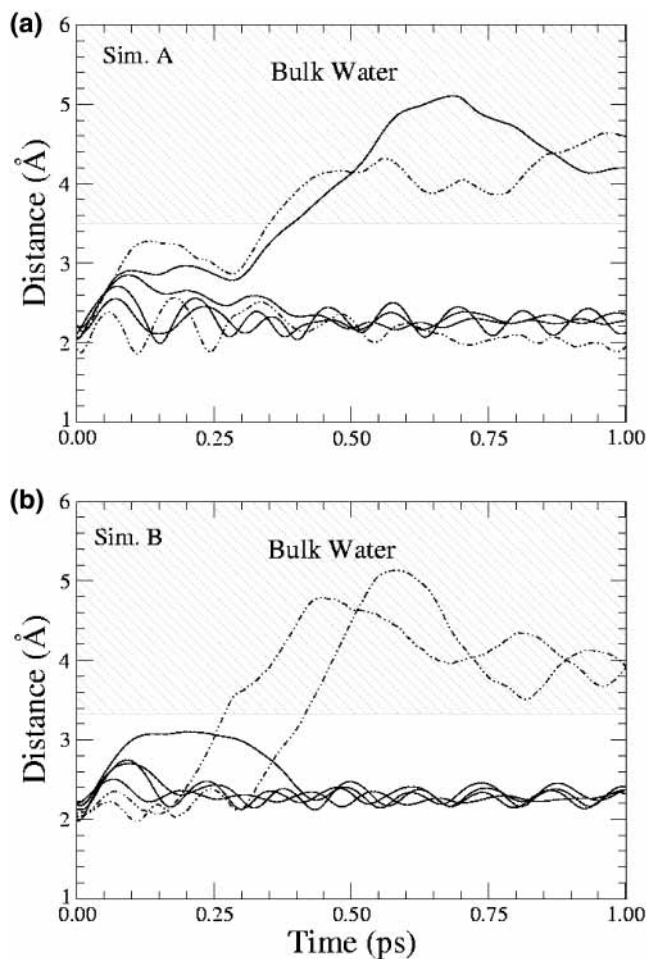


Figure 5. Calculated inter-ion distances for (a) simulation A and (b) simulation B as a function of time at 25 °C. Solid line = Zn-Cl, dash/dot = Zn-O(Cluster Water), shaded region = Zn-O(Bulk Water).

exchange of ligands around the zinc ion. Calculating this exchange rate using an ab initio approach would require long calculations in order to ensure that a large number of exchanges occur. However, this is not currently feasible with the computers available.

The change in hydration number with increasing temperature for ZnCl^+ and ZnCl_2 complexes will complicate extrapolations of solvation energies (measured at 25 °C) to hydrothermal conditions using a Born-model-based equation of state (e.g., Helgeson et al.²).

Acknowledgment. We thank the N.E.R.C. for funding (GR3/12079) and for time on the T3E at Manchester (GR9/03550).

References and Notes

- (1) Bourcier, W. L.; Barnes, H. L. *Econ. Geol.* **1987**, *82*, 1839–1863.
- (2) Helgeson, H. C.; Kirkham, D. H.; Flowers, G. C. *Am. J. Sci.* **1981**, *281*, 1249–1493.
- (3) Shock, E. L.; Oelkers, E. H.; Johnson, J. W.; Sverjensky, D. A.; Helgeson, H. C. *J. Chem. Soc., Faraday Trans.* **1992**, *88*, 803–826.
- (4) Kruh, R. F.; Standley, C. L. *Inorg. Chem.* **1962**, *1*, 941–944.
- (5) Morris, D. F. C.; Short, E. L.; Waters, D. N. *J. Inorg. Nucl. Chem.* **1963**, *25*, 975–983.
- (6) Paschina, G.; Piccaluga, G.; Pinna, G.; Magini, M. *J. Chem. Phys.* **1983**, *78*, 5745–5749.
- (7) Irish, D. E.; McCarroll, B.; Young, T. F. *J. Chem. Phys.* **1963**, *39*, 3436–3444.
- (8) Eastel, A. J.; Giaquinta, P. V.; March, N. H.; Tosi, M. P. *Chem. Phys.* **1983**, *76*, 125–128.

- (9) Ruaya, J. R.; Seward, T. M. *Geochim. Cosmochim. Acta* **1986**, *50*, 651–661.
- (10) Maeda, M.; Ito, T.; Hori, M.; Johansson, G. *Z. Naturforsch.* **1996**, *51a*, 63–70.
- (11) Tossell, J. A. *J. Phys. Chem.* **1991**, *95*, 366–371.
- (12) Parchment, O. G.; Vincent, M. A.; Hillier, I. H. *J. Phys. Chem.* **1996**, *100*, 9689–9693.
- (13) Payne, M. C.; Teter, M. P.; Allan, D. C.; Arias, T. A.; Joannopoulos,

J. D. *Rev. Mod. Phys.* **1992**, *64*, 1045–1097.

- (14) Nosé, S. *Mol. Phys.* **1984**, *52*, 255–268.
- (15) Hoover, W. G. *Phys. Rev. A* **1985**, *31*, 1695–1697.
- (16) Harris, D. J.; Brodholt, J. P.; Harding, J. H.; Sherman, D. M. *Mol. Phys.* **2001**, *99*, 825–833.
- (17) Anderson, A. J.; Mayanovic, R. A.; Bajt, S. *Can. Miner.* **1998**, *33*, 511–524.